

行政院國家科學委員會專題研究計畫成果報告

新型光電材料與光子晶體之光電物理性質研究

Studies novel photonic materials and photonic bandgap crystals

計畫編號：NSC 89-2112-M009-071

執行期限：89年8月1日至90年7月31日

主持人：謝文峰教授 國立交通大學光電工程研究所

一、中文摘要

在本報告中我們以 z-掃描法測量以雷射濺鍍製作的摻 ZnSe 微晶玻璃薄膜，用光子能量小於能隙之半的飛秒雷射脈衝測試，發現在無明顯非線性吸收之情況下，其具有相當大之光克爾係數。三階係數高達 $+0.87$ 到 $1.56 \text{ cm}^2/\text{GW}$ ，五階係數為 $+17.2 \text{ cm}^4/\text{GW}^2$ 。非線性折射率增強可能是由於接近雙光子及量子侷限效應所致。而光場引發非線性飽和之現象可以用二階光 Stark 效應來解釋。

關鍵詞： $\chi^{(3)}$ 、非線性光學、雷射濺鍍、半導體微晶玻璃。

Abstract

Large nonresonant optical Kerr coefficient without apparently nonlinear absorption was obtained from ZnSe doped glass thin films grown by pulsed laser deposition. A third nonlinear refractive index of $+0.87$ to $1.56 \text{ cm}^2/\text{GW}$ and fifth order of $+17.2 \text{ cm}^4/\text{GW}^2$ were measured for a light beam having femtosecond pulsewidth with photon energy below one half band-gap using Z-scan method. Besides the enhancement of the nonlinear refractive index results from the two-photon near resonance and quantum confinement effect, the intensity-induced saturation of nonlinear refractive index can be explained by the quadratic optical Stark shift.

Keywords: $\chi^{(3)}$, nonlinear optics, pulsed laser deposition, semiconductor doped glass.

二、緣由與目的

Since the discovery of large and fast response optical Kerr nonlinearity in semiconductor doped glass¹ (SDG) materials, intensive researches²⁻⁷ have been motivated by the applications of all-optical switching,⁸ optical computing⁹ and optical limiting.¹⁰ The nature of large nonlinearity in SDG is attributed to the quantum confinement of

electrons and holes in semiconductor nanocrystals. For example, the measured Kerr coefficient of the porous silicone shows $n_2 \sim 7.5 \times 10^{-9} \text{ esu}$ which is much larger than that of bulk silicone.¹¹ In addition, ion-implanted gold doped glass¹² has resonant $\chi^{(3)} \sim 2.5 \times 10^{-5} \text{ esu}$.

In order to optimize SDG, attempts were made to control the growth of particle size, distribution and the so-called photodarkening effect.^{4,13} Even if the exact physical mechanism of the photodarkening effect is not yet fully understood, the experiment suggests that photoexcited carriers are ejected out of the volume of quantum dots into the surface states or into the surrounding glass matrix⁴ under strong laser irradiation. The presence of carriers in the surface states resulting in change of the optical nonlinearity of material is known as the photodarkening effect. The sample with higher SiO_2 content can reduce defects and suppress the photodarkening effect,⁴ and thus the sample prepared by sol-gel method would reduce the photodarkening effect because of its good stoichiometry.

Since proposed by Sheik-Bahae et al,¹⁴ the Z-scan technique had become an important method to determine the nonlinear refractive index and nonlinear absorption of the materials. The nonlinear refractive index (γ) and two-photon absorption (TPA) coefficient (β) corresponding to the real and imaginary terms of $\chi^{(3)}$ in semiconductors could be sensitively obtained from the Z-scan profile.¹⁴ In addition, the free carrier refraction (σ) caused by two photon absorption induced carriers can also contribute to the nonlinear refraction, or the fifth-order nonlinearity, that could also be determined by measuring the Z-scan at different intensities.¹⁵ Although it was emphasized that the crystal size must be smaller than the exciton Bohr radius to

observe the quantum size effects, Cotter et al.¹⁶ has found the intense influence of quantum confinement on $\chi^{(3)}$ for the optical frequency region of $E_g/2 < h\nu < E_g$, where E_g is the bandgap and $h\nu$ the photon energy of semiconductor-doped glasses. By calculation of ΔT_{p-v} and $\Delta n/I_0$ versus the intensity considering γ and σ , the results show that the saturation would occur at relative small value of ΔT_{p-v} .¹⁷

In this paper, we report a large third and fifth order nonlinear optical properties of ZnSe doped glass thin films grown by the pulsed laser deposition from sol-gel prepared targets as excited by a femtosecond Ti:sapphire laser. Since the blue-shifted bandgap of the SDG quantum dots is larger than twice of the incident photon energy, the ZnSe SDG do not show nonlinear absorption but have Kerr coefficient of $+0.87$ to $1.56 \times 10^{-9} \text{ cm}^2\text{W}^{-1}$ or $+5.18$ to 9.29×10^{-7} esu and the fifth order nonlinear coefficient of $1.72 \times 10^{-17} \text{ cm}^4\text{W}^{-2}$ measured by the z-scan transmittance.

三、實驗方法與步驟

A. Sample preparation

The detailed SDG thin films prepared by pulsed laser deposition from sol-gel targets had been discussed in our previous works,¹⁸⁻²⁰ and will be briefly described as below. The targets were fabricated by the sol-gel processes with molar ratio of ZnSe:SiO₂ = 1:6. The growth of thin films was carried out in a high vacuum system with a base pressure of about 5×10^{-5} Torr and using a 1 mm thick fused silica plate as substrate. High-purity SiO₂ doped with ZnSe nanocrystallite thin films were grown by vaporizing the target with a 10-mJ KrF excimer laser (ATL-15). The laser operates at wavelength of 284 nm with pulse width 7 ns and repetition rate 50 Hz. In order to ensure that the laser beam vaporized the target uniformly and efficiently, the laser beam was focused to a spot of diameter 0.3 mm on the target, which was mounted onto a small rotating motor. The substrate was located 3 cm away from the target at room temperature. The as-grown film thickness was measured by an ellipsometer as 300 nm.

B. Measurements of linear and nonlinear optical properties

To determine the bandgap of the prepared ZnSe-SDG thin films, we have

measured the transmittance of the samples, respectively by using HP8453 UV-visible spectrometer with wavelength scanned from 190 to 1100 nm at room temperature. And room-temperature photoluminescence of the samples was measured by the ARC SpectrPro-500 spectrometer with a He-Cd laser (wavelength 325 nm) as excitation source.

The standard Z-scan measurement was performed by a KLM Ti:sapphire laser that operates at 790 nm with its pulsewidth 80 fsec at 93.3 MHz repetition rate. A lens of 5 cm focal length was used to focus the laser beam onto the tested sample and then the transmitted light through an aperture is detected by a photoconductive p-i-n diode. At different pump intensities, the transmittance was measured as a function of position z by scanning the sample through the z -direction with an opened aperture ($S=1$) and a closed aperture ($S=0.36$), separately. Thus, the nonlinear refractive index and absorption were obtained accordingly.¹⁵

四、結果與討論

The transmission spectrum indicates a typical 300 nm thick ZnSe-SDG film has transmittance of almost 95% over 600nm to 1000 nm wavelength range. The converted absorption coefficient versus the energy is shown in Fig. 1 that indicates $\alpha = 1.64 \times 10^5 \text{ m}^{-1}$ at the pump wavelength $\lambda = 790 \text{ nm}$ (or 1.57 eV). The transmission and PL spectra show that the samples have band gap about 3.25 eV (or 382 nm). It shows large blue shift of bandgap about 0.5 eV corresponding to the crystal size around 3 nm,^{18,19} which is consistent with the report by Smith et al.²¹

Some of the Z-scan traces over the different pumping irradiance from 0.08 GW/cm² to 1.04 GW/cm² are shown in Fig. 3. The irradiance is estimated through the focusing spot size $w_p=32 \mu\text{m}$ measured with a knife-edge method at the focal point of the pump lens. For example, the estimated irradiance 1.04 GW/cm² corresponds to the average input power of 250mW. Note that the measured spot size (w_p) is very closed to the value of 26.5 μm obtained from separation of peak and valley of the normalized Z-scan transmission curve to be $1.7z_0$, where $z_0 = (\pi w_p^2/\lambda) \sim 2.8 \text{ mm}$ is the confocal parameter of the focused gaussian beam.^{14,15}

A typical Z scan data with open aperture ($S=1$) and closed aperture ($S=0.36$) are displayed in Fig. 1, the samples act as self-

focusing ($n_2 > 0$) materials due to the feature of valley-peak characterization and without nonlinear absorption even with the pump irradiance as high as 1.04 GW/cm^2 . It can be seen by the open aperture Z-scan in which shows almost a straight line with fluctuation due to the detection noise from detector and circuitry. We conducted the experiment from the highest irradiance to the lowest one then back up. Within about 2-hour exposure to the laser irradiation, another measurement with the normalized transmittance difference at 1.04 GW/cm^2 . By fitting the Z-scan data without considering nonlinear absorption ($\beta=0$) using Eq. (1), the $\Delta T_{p-v}=0.223$ as compared with $\Delta T_{p-v}=0.219$ measured after 2 hour irradiation shows no apparent photodarkening effect.

The normalized transmittance difference ΔT_{p-v} as a function of the pump irradiance I are summarized in Fig. 2. Initially ΔT_{p-v} increases almost linearly and then decreases when the pump irradiance exceeds 0.17 GW/cm^2 . It is different from those results that either saturates to a constant due to converting to the fifth-order nonlinear refraction¹⁷ or linearly decreases caused by the optical Stark effect^{22,23} in the frequency region $E_g/2 < h\nu < E_g$. Thus, some other effects may be involved besides saturation due to exciting the fifth order nonlinearity for high pump.

Since single photon energy of the pump source is 1.57 eV , even with two-photon energy 3.14 eV is still below the bandgap of the samples of 3.2 eV (or 3.25 eV determined from absorption) as aforementioned. Therefore, the nonlinear absorption including two-photon and excited state absorption will not take place. It is well-known that when the incident photon energy satisfies $h\nu < E_g/2$, the nonlinear refraction is mainly caused by cascade two-photon or quadratic optical Stark process of the bound electrons that can be expressed as the first term of the relation²⁴

$$\chi_{1111}^{(3)} \approx \frac{2N}{3\hbar^3} \left[\ddot{y}_{lmn} \frac{\mu_{gn}^x \mu_{nm}^x \mu_{ml}^x \mu_{gl}^x}{(\omega_{ng} > \omega)(\omega_{mg} > 2\omega)(\omega_{lg} > \omega)} \right. \\ \left. > \ddot{y}_{ln} \frac{\mu_{gn}^x \mu_{ng}^x \mu_{lg}^x \mu_{gl}^x}{(\omega_{ng} > \omega)(\omega_{lg} > \omega)(\omega_{lg} > \omega)} \right]$$

A similar term including two-photon resonant denominator can also be found in the expression for the fifth-order susceptibility. An atom or an ion may increase its probability of residing in the excited state to increase the effective polarizability in the present of an applied optical field²⁴, that is, the nonlinear refractive index change is positive and is consistent with our Z-scan observation with $n_2 > 0$.

Further enlarging the pump intensity causes the near two-photon resonant energy levels to split further away due to the quadratic Stark shift²⁴, so as to reduce the nonlinear coefficients $\chi^{(3)}$ and $\chi^{(5)}$. Therefore, we will consider the saturation as a function of $(I_0/I_s)^2$ rather than (I_0/I_s) , where I_s is the saturation intensity. To best fit the experimental result, we have used the relation,

$$\Delta T_{p-v} = A \frac{AI_0 + I_0^2}{\left(\frac{I_0 - I_{th}}{I_s}\right)^2 + 1},$$

to consider pump saturation of nonlinear refractive index through the quadratic optical Stark shift, where the proportion constant $A = 0.406(1-S)^{0.25} kL_{\text{eff}}/\sqrt{2}$ with I_0 being the incident intensity at the center of the beam and $L_{\text{eff}} = (1-e^{-\alpha L})/\alpha$ the effective length of the sample.¹⁵ The fitting curve also shown as thin line in Fig. 2 has less than 2% deviation with the third-order coefficient $\gamma = +0.87 \text{ cm}^2/\text{GW}$, the fifth-order coefficient $\sigma = +17.2 \text{ cm}^4/\text{GW}^2$, the saturation intensity $I_s = 0.13 \text{ GW/cm}^2$, and an undefined threshold intensity $I_{th} = 79 \text{ MW/cm}^2$, that will be discussed below. We also evaluated γ from the slope of linear region,¹⁵ with $\Delta T_{p-v} \sim 0.1-0.2$, to be $\gamma = +1.56 \text{ cm}^2/\text{GW}$ or $n_2 = +9.29 \times 10^{-7} \text{ esu}$. Either one of the results is much larger than the resonant result $n_2 = -4.4 \times 10^{-11} \text{ esu}$ for 2.7 mm -thick ZnSe bulk at 532 nm .¹⁵

Although it was known that no

threshold behavior was included for the quadratic Stark shift, we had obtained the threshold intensity for fitting the saturation of the nonlinear susceptibility. We think that the threshold intensity may be somehow related to the self-trapping of the optical beam within the SDG films. By using $\gamma = +0.87 \text{ cm}^2/\text{GW}$ and $w_p = 30 \text{ }\mu\text{m}$, we estimated the self-trapping intensity to be order of $20 \text{ kW}/\text{cm}^2$ for thick samples which is a lot less than the obtained result with $I_{th} = 79 \text{ MW}/\text{cm}^2$ for our 300 nm ZnSe-SDG films.

六、自我評估

上年度報告中以 X 光繞射和拉曼光譜研究溶膠凝膠法製備一系列鈦酸鋇鈾的微晶粉末，在 $x \sim 0.45$ 時新發現排列秩序相變之結果已發表於 Physical Rev. B 中。本年度之報告也以撰文投稿中。除了報告內容外，我們也以雷射濺鍍成功地成長並研究 GaSe 和 Ga_2Se_3 單晶薄膜。由拉曼與 X 光繞射在沒有表面鈍化處理情況下，我們發現由於 GaSe 為分子層狀晶體結構的特性，在 2D-3D 長晶條件下，成長 80nm 的厚度就能完全消除介面之應力。我們也提出觀察 TO 拉曼震盪模可以有效的檢測應力效應。此結果正撰文投稿中。本年度之研究大致依計劃進度進行。

七、結論

We have determined the nonlinear susceptibilities $\chi^{(3)}$ and $\chi^{(5)}$ of the ZnSe-SDG film from the pump intensity dependent Z-scan measurement. While the incident photon energy being less than one-half bandgap of ZnSe-SDG films, no apparent nonlinear absorption was found at the open aperture Z scan trace but large nonlinear positive refraction index was measured at the close aperture due to the quantum confinement effect and two photon near resonant. The positive third and fifth order nonlinear coefficients as large as 0.87 to $1.56 \text{ cm}^2/\text{GW}$ and the fifth order of $17.2 \text{ cm}^4/\text{GW}^2$ are obtained by fitting with the Z scan transmittance versus the incident power. The fitting function shows the saturation of nonlinear refraction is reciprocal of quadratic power of the incident to saturation intensity ratio together with a threshold intensity that may be accounted for the quadratic Stark shift with possible self-trapping effect in the medium.

八、參考文獻

1. R.K. Jain and R.C. Lind, "Degenerate four-wave mixing in semiconductor

doped glasses," J. Opt. Soc. Am 73, 647-653 (1983).

2. D. Cotter, H. P. Girdlestone and K. Moulding, "Size-dependent electroabsorptive properties of semiconductor microcrystallites in glass," Appl. Phys. Lett. 58, 1455-1457 (1991).
3. P.E. Lippens and M. Lannoo, "Calculation of the band-gap for small CdS and ZnS crystallites," Phys. Rev. B 39, 935-942 (1989).
4. K. Kang, A.D. Kepner, "Room temperature spectral hole burning and elimination of photodarkening in sol-gel derived CdS quantum dots," Appl. Phys. Lett. 64, 1487-1489 (1994).
5. D. Nesheva, C. Raptis, Z. Levi, Z. Popovic, I. Hinic, "Photoluminescence of CdSe nanocrystals embedded in a SiO_x thin film matrix," J. Lumin. 82, 233-240 (1999).
6. M. Nikl, K. Polak, and J. Rosa, "CuCl quantum dots in CuCl-doped nanocrystals," Solid State Commun. 85, 467-470 (1993).
7. Y. Nakata, Y. Sugiyama, and M. Sugawara, "Molecular beam epitaxial growth of self-assembled InAs/GaAs quantum dots," Semiconduct. Semimet. 60, 117-154 (1999).
8. J. H. Kim, K.R. Oh, H.S. Kim, et al, "All-optical switching by counterpropagating operation in cascaded semiconductor optical amplifiers," IEEE Photonic Tech. Lett. 12, 513-515 (2000).
9. I. R. Jones, V. P. Heuring, "Simulating Free-Space Optical Computing Architectures," Appl. Optics 37, 6127-6135 (1998).
10. J. Hecht, "Optical limiter attenuates intense laser pulses," Laser Focus World 32, 37-38 (1996).
11. F. Z. Henari, K. Morgenstern, W. J. Blau, J. V. A. Karavanskii, V. S. Dneprovskii, "Third-order optical nonlinearity and all-optical switching in porous silicon," Appl. Phys. Lett. 67, 323-325 (1995).
12. H. B. Liao, R. F. Xiao, J. S. Fu, P. Yu, G. K. L. Wong, P. Sheng, "Large third-order optical nonlinearity in Au:SiO₂ composite films near the percolation threshold," Appl. Phys. Lett. 70, 1-3 (1997).
13. J. Malhorta, D. J. Hagan, and B. G. Potter, "Laser-induced Darkening in

- semiconductor-doped glasses,” J. Opt. Soc. Am. B 8, 1531-1536 (1991).
14. M. Sheik-Bahae, A. A. Said, T. H. Wei, D. J. Hagan, E. W. Van Stryland, “Sensitive measurement of optical nonlinearities using a single beam, IEEE J. Quantum Electron. 26, 760-769 (1990).
 15. A. A. Said, M. Sheik-Bahae, D. J. Hagan, T. H. Wei, J. Wang, J. Young, E. W. Van Stryland, “Determination of bound-electronic and free-carrier nonlinearities in ZnSe, GaAs, CdTe, and ZnTe,” J. Opt. Soc. Am. B 9, 405-414 (1992).
 16. D. Cotter, M. G. Burt, and R. J. Manning, “Below-band-gap third-order optical nonlinearity of Nanometer-size semiconductor crystallites,” Phys. Rev. Lett. 68, 1200-1203 (1992).
 17. K.S. Bindra, S.M. Oka, “Intensity dependence of Z-scan in semiconductor-doped glasses for separation of third and fifth order contributions in the below band gap region,” Opt. Commun. 168, 219-225 (1999).
 18. S. B. Yin, W. F. Hsieh, “Fabrication and characterization of CdS nanostructure doped glass thin films grown by pulsed laser evaporation,” Jpn. J. Appl. Phys. 36, 5646-5650 (1997).
 19. S. B. Yin, Lisa Chen and W. F. Hsieh, “Fabrication and Raman analysis of ZnSe quantum dots in glass matrix thin films by pulsed laser evaporation,” Jpn. J. Appl. Phys. 37, 4154-4157 (1998).
 20. J. C. Jan, S. Y. Kuo, S. B. Yin and W. F. Hsieh, “Temperature Induced Stress of ZnSe Quantum Dots in Glass Matrix Thin Films Grown by Pulsed Laser Deposition,” Chinese J. Phys. 39, 90-97 (2001).
 21. C. A. Smith, H. W. H. Lee, V. J. Leppert and S. H. Risbud, “Ultraviolet-blue emission and electron-hole states in ZnSe quantum dots,” Appl. Phys. Lett. 75, 1688-1690 (1999).
 22. B.L. Yu, C.S. Zhu, and F.X. Gan, “Nonlinear optical absorption and refraction by CdTe microcrystals doped in glass,” J Appl. Phys. 87, 1759-1761 (2000).
 23. I. H. Ishihara and K. Cho, “Enhancement of the third-order nonlinear optical response of quantum wells in a semiconductor microcavity,” Appl. Phys. Lett. 73, 1478-1480 (1998).
- R. W. Boyd, *Nonlinear Optics*, p176,

Academic Press (1992).

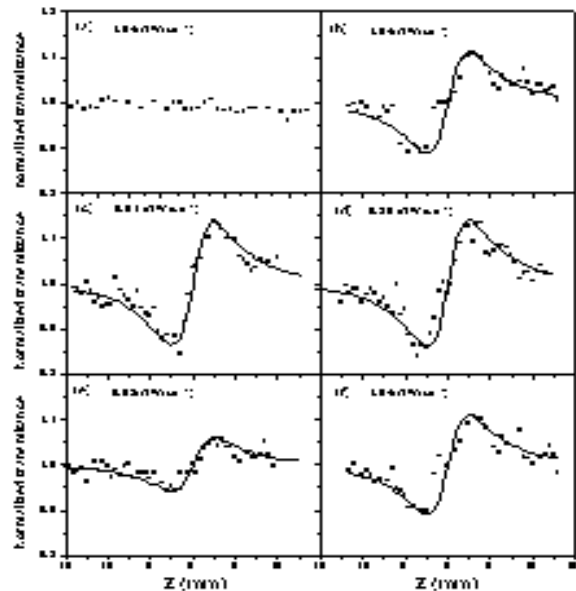
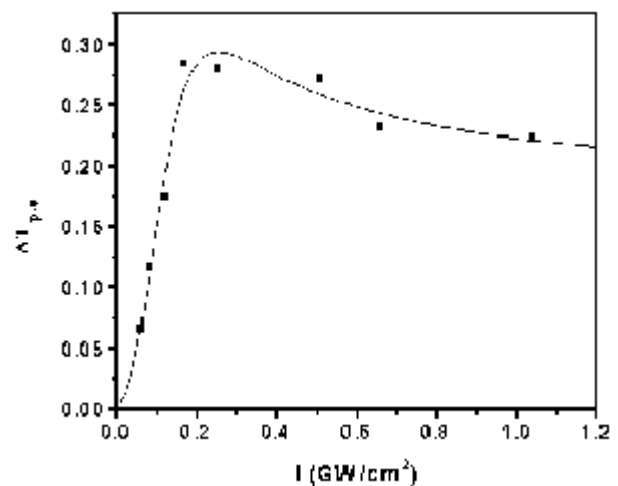


Fig. 1 Pump intensity dependent Z-scan normalized transmittance. The pump intensity is indicated in the figure.
Fig. 2 Plot of normalized transmission



difference versus pump intensity with dotted points representing experimental data and the curve fitted with quadratic intensity dependent saturation.

